Bioorganic Chemistry **29,** 211–222 (2001)
doi:10.1006/bioo.2001.1214, available online at http://www.idealibrary.com on IDEAL®

Inhibition and Structure–Activity Studies of Methionine Hydroxamic Acid Derivatives with Bacterial Peptide Deformylase

Stephan K. Grant,*,[1] Barbara Gordon Green,† and John W. Kozarich†

**Department of HTS and Automation and †Department of Biochemistry Merck & Co., P.O. Box 2000, Rahway, New Jersey 07065*

Received February 1, 2001; published online August 9, 2001

The posttranslational deformylation of *N*-formyl-Met-polypeptides by the metalloenzyme, peptide defomylase, is essential for bacterial growth. Methionine hydroxamic acid derivatives were found to inhibit recombinant *Escherichia coli* peptide deformylase activity containing either zinc or cobalt. The binding of methionine hydroxamate and hydrazide inhibitors to cobalt-substituted deformylase caused spectral changes consistent with the formation of a pentacoordinate metal complex similar to that of actinonin, a psuedopeptide hydroxamate inhibitor. The spectral and kinetic data support the binding of these *N*-substituted L-methionine derivatives in a reverse orientation with respect to *N*-formyl-Met-peptide substrates within the active site. Based on this hypothesis a second generation of *N*-substituted methionyl hydroxamic acids were evaluated and found to possess greater inhibitory potency. These results may provide the basis for the design of more potent and selective deformylase inhibitors as potential antibacterial agents.

Key Words: peptide deformylase; metalloenzyme; hydroxamic acid; hydrazide; actinonin; enzyme inhibition.

INTRODUCTION

Bacteria contain many aminopeptidases that cleave N-terminal amino acids from peptides. Methionine aminopeptidase (MetAP, EC 3.4.11.18), for example, is an essential bacterial enzyme that hydrolyzes Met from polypeptides during protein maturation (*1*,*2*). MetAP cannot hydrolyze N-blocked Met-polypeptides such as *N*-formyl-Met-peptide formed during protein synthesis in eubacteria (*3*). Deformylation of the *N*-formyl-Met-polypeptide is therefore a prerequisite step for proper posttranslational modification of eubacterial proteins. The deformylation step is catalyzed by

[1] To whom correspondence should be addressed. Department of HTS and Automation, Merck Research laboratories, RY80N-1B28, P.O. Box 2000, Rahway, NJ 07065. Fax: (732) 594-0390. E-mail: stephan__grant@merck.com.

[2] Abbreviations used: fMV, *N*-formyl-Met-Val; LMCT, ligand to metal charge transfer; MetAP, methionine aminopeptidase; PDF, peptide deformylase.

0045-2068/01 $35.00

the bacterial metalloenzyme, peptide deformylase (PDF, EC 3.5.1.27). *Escherichia coli* PDF contains a metal binding motif HEXXH, which is conserved among deformylase sequences from diverse bacterial sources (*4–6*). A Cys-thiolate is also conserved in the active site, forming a tetracoordinate metal center with two imidazole groups from the HEXXH motif and a catalytic water molecule (*4,5*). Several metals including zinc (*7,8*), cobalt (*8*), nickel (*9,10*), and iron (*1,12*) have been found in preparations of purified recombinant *E. coli* PDF. The specific activity of the enzyme changes greatly depending upon which metal ion is bound within the active site. Cobalt (*8*) and nickel (*9,10*) enzymes have much greater k_{cat}/K_m values for *N*-formyl-Met-peptides such as the chemotactic peptide, *N*-formyl-Met-Leu-Phe (10^3–10^5 M^{-1} s^{-1}), than zinc-PDF (10^2–10^3 M^{-1} s^{-1}). The variation of specific activity with different metal substitution has been attributed to the turnover of substrate, a k_{cat} effect, rather than substrate binding affinity (*8*). While the iron-enzyme is more active than other metal-substituted deformylases (10^4–10^6 M^{-1} s^{-1}), its activity is also much less stable (*8,11–13*).

The initial characterization of recombinant zinc *E. coli* peptide deformylase by commercially available *N*-formylated peptides such as *N*-formyl-Met-Leu-Phe, indicated that the enzyme was specific for *N*-formylated-Met-peptides or *N*-formyl-norleucine peptides (*7*). The solution NMR (*16*) and crystal structures (*17,18*) of recombinant *E. coli* PDF indicated that the active site is buried within the protein. From these structural studies a model was proposed where *N*-formyl-peptide substrates may enter the active site but not extend beyond the metal binding pocket. This restricted active site model provides an explanation for why PDF hydrolyzes formamide substrates and lacks peptidase activity (*7*).

While the zinc-enzyme appears to be selective for *N*-formylated-Met-peptides, studies with nickel-PDF (*14*) and iron-PDF (*15*) has extended the substrate specificity to include *N*-formylated peptides with hydrophobic aromatic amino acids at the P1′ position, such as *N*-formyl-Phe-Ala-Ser. It has also been reported that *N*-difluoroacetyl-Met-Leu-*p*-nitroanilide and *N*-trifluoroacetyl-Met-Leu-*p*-nitroanilide but not *N*-acetyl-Met-Leu-*p*-nitroanilide can be deacetylated by iron-PDF (*15,19*). Furthermore, our laboratory has recently reported that peptide aldehydes (*8*) and biaryl acid analogs (*20*) are also inhibitors of recombinant deformylase but are more potent against cobalt-substituted PDF than the zinc-enzyme. Together the results from these separate studies suggest that deformylase substrate and inhibitor selectivity may be dependent upon which metal is bound within the enzyme active site. Metal-dependent inhibitor selectivity may be an important consideration in the design and development of PDF inhibitors as potential antibacterial agents.

Recently, the antibiotic activity of actinonin **1**, a pseudopeptide hydroxamic acid, was shown to be attributable to its specific inhibition of peptide deformylase (*21*). Actinonin was also found to be a very potent inhibitor of recombinant zinc, nickel, and iron-substituted *E. coli* deformylase (*21*). In this study, we have evaluated the activity and binding characteristics of a series of methionine hydroxamic acid derivatives against recombinant *E. coli* deformylase specifically containing either zinc or cobalt.

EXPERIMENTAL PROCEDURES

Materials. Actinonin **1** and *N*-formyl-Met-Val were obtained from Sigma (Fig. 1). *N*-[4-(Trifluoromethyl)benzoyl]-L-methionine hydroxamic acid **2**, *N*-[4-(trifluoromethyl)-benzoyl]-L-methionylhydrazide **3**, and *N*-[4-(Trifluoromethyl)benzoyl]-L-methionine methyl ester **4** were purchased from Maybridge Chemical Company (Cornwall, UK). The enantiomeric purity of the commercially obtained compounds **1–4** was confirmed by ^{1}H NMR (J. O'Connell, Merck & Co., pers. commun.). The second generation methionyl hydroxamic acids were procured from Pharm-Eco Laboratories, Inc. (Lexington, MA). The compounds were synthesized by coupling various carboxylic acids to DL-methionyl hydroxamic acid with an average 85% purity with none less than 70% purity (Richard Lombardy, Pharm-Eco Laboratories, Inc., pers. commun.).

Preparation of enzymes. The cloning, expression, and purification of recombinant truncated and full-length *E. coli* PDF was previously described (*8,16*). For production of recombinant deformylase with homogeneous metal content, bacterial cells were grown in media with defined metal sources that provided recombinantly expressed deformylase specifically containing either zinc or cobalt (*16*). Similar K_m values for *N*-formyl-Met-Val were determined for truncated zinc and cobalt deformylase of 8.0 $\pm$ 0.2 and 7.1 $\pm$ 0.3 mM, respectively. A K_m value of 12.4 $\pm$ 0.8 mM was determined for the full-length cobalt enzyme with *N*-formyl-Met-Val. Metal content of homogeneous metal-substituted enzymes was confirmed by inductively coupled plasma mass spectrometry (T. Wang, Analytical Research, Merck & Co., pers. commun.) or atomic

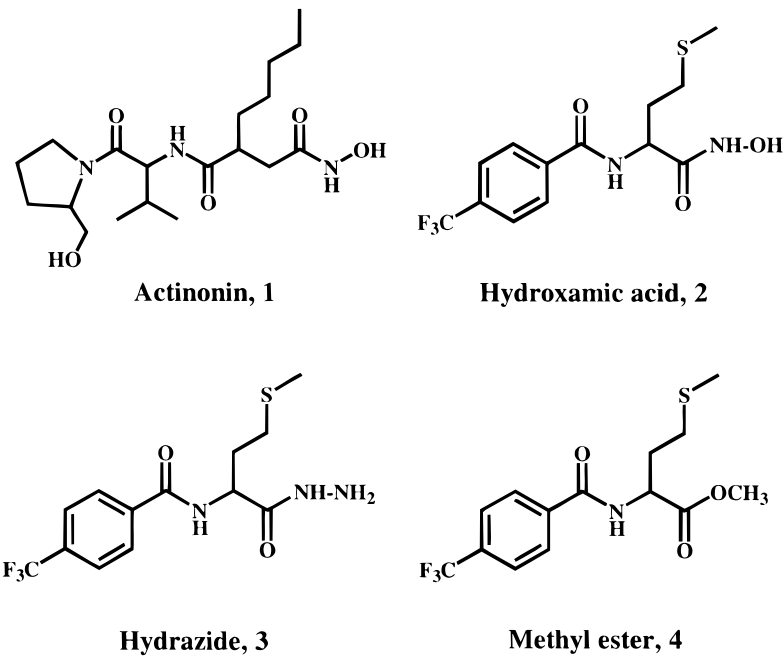

FIG. 1. Structures of Actinonin and *N*-benzoyl-methionine analog derivatives.

absorption spectrophotometry (Schwarzkopf Microanalytical Laboratory, Woodside, NY).

Enzyme activity assays. Deformylase activity was monitored by a NAD-formate dehydrogenase coupled, continuous spectrophotometric assay as described earlier (*8*). IC_{50} values were determined in duplicate from initial velocity measurements at varying inhibitor concentrations and a single substrate concentration (2 mM *N*-formyl-Met-Val). Reversibility was evaluated by preincubation of enzyme and inhibitor followed by dilution into an assay buffer containing saturating substrate (40 mM *N*-formyl-Met-Val). The kinetic mechanism of enzyme inhibition was evaluated by varying inhibitor and substrate concentrations and fitting initial velocity data to equations for competitive, noncompetitive, and uncompetitive inhibition. Time-dependent inhibition was evaluated by fitting nonlinear progress curves to the integrated first-order expression, $y = v_s t + (v_0 - v_s)(1 - e^{-kt})/k_{obs} + A_0$, where v_s is the steady-state velocity, v_0 is the initial velocity, and k_{obs} is the observed rate constant. Kinetic parameters for slow-binding enzyme inhibition were determined from plotting the observed rate constants versus inhibitor concentration according to $k_{obs} = k_{on}[I] + K_{off}$ and $K_I = k_{off}/k_{on}$, where k_{on} is the association rate constant, I is the inhibitor concentration, k_{off} is the dissociation rate constant, and K_I is the inhibitor equilibrium dissociation constant.

Electronic absorption spectra. Optical spectra of cobalt-substituted deformylase were measured with a Hewlett Packard diode array spectrophotometer (Model HP8452A) equipped with a thermojacketed cell holder and circulating water bath. Samples (0.3 mL) were incubated at 25°C and the addition of concentrated inhibitors were made with a Hamilton 10-μL syringe to minimize sample dilution. Spectra were recorded before the addition of inhibitor to the protein solution and then after subsequent additions of inhibitor. The samples were allowed to equilibrate between addition of compounds and the spectral signals were stable after 1 min. The difference spectrum was generated by subtraction of the spectrum of the protein before the addition of compound.

RESULTS

Inhibition of peptide deformylase by N-benzoyl-methionine derivatives. Three *N*-benzoyl-methionine derivatives: *N*-[4-(Trifluoromethyl)benzoyl]-L-methionine hydroxamic acid **2**, *N*-[4-(trifluoromethyl)benzoyl]-L-methionyl hydrazide **3**, and *N*-[4-(trifluoromethyl)benzoyl]-L-methionine methyl ester **4**, were examined as potential deformylase inhibitors at 1 mM. Both the hydroxamate **2** and hydrazide **3** inhibited both zinc and cobalt-substituted PDF activity, but the methyl ester **4** did not. In support of the proposal that the observed inhibition of PDF by compounds **2** and **3** was specific and not via chelation or inhibition of the coupling enzyme, we demonstrated that the inhibition of PDF was unaffected by addition of free zinc or cobalt (0.1 mM) and that these compounds did not inhibit formate dehydrogenase alone. The hydroxamic acid **2** was a more potent inhibitor of Co-PDF than Zn-PDF with IC_{50} values of 3.2 $\pm$ 0.2, 37.0 $\pm$ 0.7, and 330 $\pm$ 30 μM for truncated and full-length Co-PDF and truncated Zn-PDF, respectively. The inhibition of full-length Co-PDF by hydroxamic acid **2** was competitive with $K_i = 30.0 \pm 1.1$ μM (Fig. 2). In contrast, actinonin **1** gave complete inhibition of *E. coli* PDF activity when assayed at 1 μM. An accurate IC_{50} value for actinonin against zinc or cobalt deformylase could not be

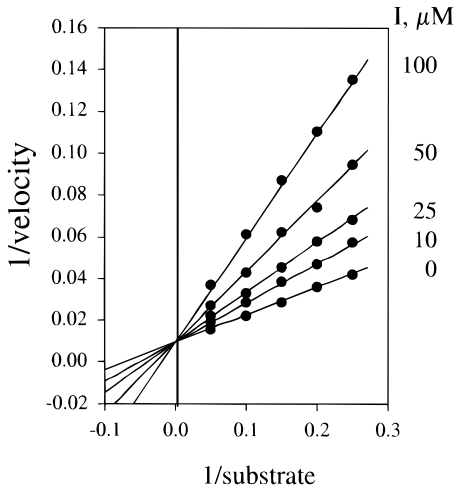

FIG. 2. Double-reciprocal plot for inhibition of Co-PDF by (4-[trifluoromethyl]benzoyl)-L-methionine hydroxamic acid **2** (0, 10, 25, 50, or 100 μM). Experiment was performed in duplicate and average values are shown. Substrate concentration was 4, 5, 6.6, 10, or 20 mM fMV. Velocity data (mOD/min) was fit to a competitive model of inhibition by a nonlinear least-squares algorithm.

determined because actinonin still inhibited enzyme activity at concentrations equal to the lowest enzyme concentration that can be accurately detected by the spectrophotometric assay (about 1 nM for Co-PDF and 30 nM for Zn-PDF). This is consistent with a recent report (*21*) that estimated a K_i value of 0.25 nM for actinonin with recombinant Ni-PDF.

Unlike hydroxamate **2**, hydrazide **3** displayed time-dependent inhibition of zinc and cobalt deformylase. Representative plots of the time-dependent inhibition of PDF by the hydrazide are shown in Fig. 3 and were observed when assayed at substrate concentrations (40 mM fMV) greater than K_m. The inhibition curves were psuedo-first-order and were observed when the reaction was initiated with either enzyme or substrate. When the reaction was initiated with enzyme in the presence of hydrazide **3**, there was a fast initial velocity for product formation followed by a slower steady-state velocity. This inhibition was fully reversible, since preincubation of enzyme with inhibitor followed by the addition of excess substrate gave a slow initial velocity that changed to a faster steady-state velocity. For both experiments the steady-state velocities were nearly identical. Kinetic parameters for the time-dependent inhibition were determined by fitting the data to the integrated first-order expression. A plot of the observed rate constants versus inhibitor concentration is shown in Fig. 4. The data fit best to a model mechanism for slow-binding enzyme inhibition and gave slow association rates (k_{on} values) for the binding of the inhibitor to the enzyme. The kinetic parameters for the time-dependent inhibition of truncated and full-length PDF by hydrazide **3** are shown in Table 1. The kinetic parameters for the slow-binding inhibition of the truncated Zn and Co-enzymes were very similar but the association rate of the hydrazide was slower with full-length Co-PDF. Spectral studies were

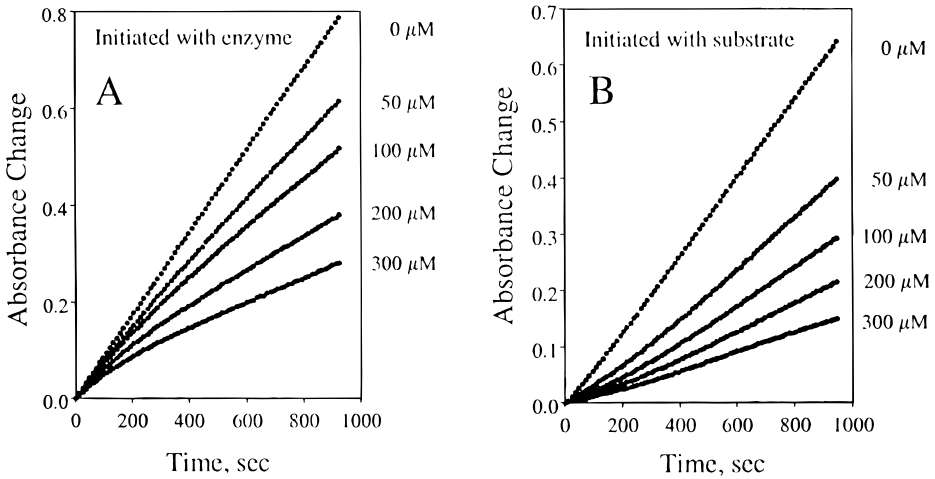

FIG. 3. Slow-binding kinetics for inhibition of PDF by hydrazide **3**. (A) Representative time courses for the enzyme reaction in the presence of inhibitor when initiated by enzyme. Inhibitor concentration was 0, 0.05, 0.1, 0.2, and 0.3 mM with 40 mM fMV. (B) Representative time courses for the enzyme reaction after preincubation with inhibitor for 20 min at 25°C, followed by initiation with 40 mM fMV. Experiments were performed in triplicate with average values shown.

initiated with cobalt-substituted PDF to further evaluate the binding of the hydroxamate and hydrazide inhibitors.

Electronic spectra for inhibitor binding to cobalt-peptide deformylase. Cobalt-substituted full-length and truncated *E. coli* deformylase were pink-colored proteins (*8*). Distinct spectral bands were observed for both cobalt-substituted enzymes at about 330, 562, and 660 nm (partially obscured by an instrument spike). These bands

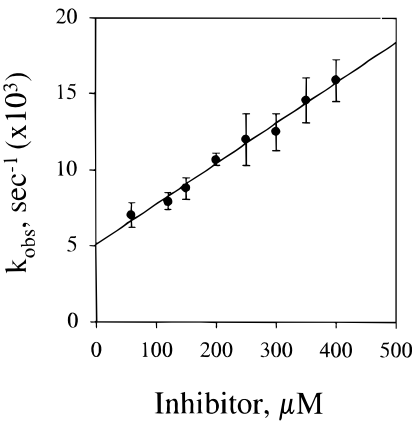

FIG. 4. Plot of observed rate constants versus inhibitor concentration for time-dependent inhibition of PDF by hydrazide **3**. Observed rate constants were calculated by fitting inhibition curves to the integrated first-order expression. Values were averaged from triplicate experiments with standard deviations shown.